ULTRA-FAST OLEOPHOBIC–HYDROPHILIC SWITCHING SURFACES FOR ANTI-FOGGING, SELF-CLEANING, AND OIL–WATER SEPARATION

P. S. Brown, O. D. L. A. Atkinson, and J. P. S. Badyal*

Department of Chemistry
Science Laboratories
Durham University
Durham DH1 3LE
England, UK

* Corresponding author email: j.p.badyal@durham.ac.uk

ABSTRACT

Smooth copolymer–fluorosurfactant complex film surfaces are found to exhibit fast oleophobic–hydrophilic switching behaviour. Equilibration of high oil contact angle (hexadecane = 80°) and low water contact angle (<10°) values occurs within 10 s of droplet impact. These optically transparent surfaces display excellent anti-fogging and self-cleaning properties. The magnitude of oleophobic–hydrophilic switching can be further enhanced by the incorporation of surface roughness to an extent that it reaches a sufficiently high level (water contact angle <10° and hexadecane contact angle >110°) which, when combined with the inherent ultra-fast switching speed, yields oil–water mixture separation efficiencies exceeding 98%.

Keywords: Oleophobic–hydrophilic; switching surface; anti-fogging; self-cleaning; oil–water separation; copolymer–fluorosurfactant complex.

1. INTRODUCTION

Due to the frequency of off-shore oil spillages,[1,2] and the emergence of fracking (where water-based fluids are used to fracture rocks for the release of oil and gas), the separation of oil and water is an important environmental challenge.[3,4,5,6,7,8] Existing methods for the removal or collection of oils from an oil–water mixture utilise absorbent materials[9] such as zeolites,[10,11] organoclays,[12] non-woven polypropylene,[13,14] or natural fibres[15] (such as straw,[16] cellulose,[14] or wool[17]). However, these materials also tend to absorb water, thereby lowering their efficiency.[18] In addition, extra steps are necessary in order to remove the absorbed oil from the material, which makes such methods highly incompatible with continuous flow systems (e.g. attached to clean-up marine vessels). There also exist separation membranes that repel one liquid phase whilst allowing the other to pass through. Typically these are made out of hydrophobic and oleophilic materials,[19,20,21] causing water to run off the surface whilst allowing oil to permeate through. Their main drawback tends to be surface contamination with oil culminating in a drop in separation efficiency.[22,23] The most attractive approach to date appears to be the utilisation of oleophobic–hydrophilic surfaces where the oil and oil-based contaminants are repelled and water passes through.[24] Such surfaces are also of interested for self-cleaning,[25,26,27] anti-fog,[25,28,29] and anti-fouling[30,31] applications.

One important class of oleophobic–hydrophilic surfaces are polyelectrolyte–surfactant complexes,[32,33] where the surfactant is attached to the polyelectrolyte via an oppositely charged electrostatic interaction.[34,35] In the case of polyelectrolyte–fluorosurfactant complexes, the fluorinated alkyl chains can orientate towards the air–solid interface to provide a low surface energy film. Such alignment localises hydrophilic portions of the polyelectrolyte in the near-surface region due to electrostatic attraction.[36] This means that when water is placed onto the surface, it penetrates through defects in the fluorinated outermost layer towards the hydrophilic sub-surface, giving rise to a “switch” of the surface–water interaction from hydrophobic to hydrophilic.[37] Larger oil molecules are unable to penetrate through this top layer leaving the surface oleophobic.[37] Earlier polyelectrolyte–surfactant complex oleophobic–hydrophilic surfaces have been impeded from more widespread usage due to several factors: it can take several minutes for the water to penetrate through the fluorinated top layer, resulting in a surface that is initially

hydrophobic;[38,39] and the level of oil repellency is quite poor, (hexadecane contact angles of only 70° or lower[40,41,42]). Pulsed plasma deposited poly(maleic anhydride) and poly(acrylic acid) surfaces that are subsequently complexed to fluorosurfactant display better oleophobicity,[32,33] however the two step process is unsuitable for many large scale industrial applications.

In this study, fast-switching oleophobic–hydrophilic polyelectrolyte–fluorosurfactant surfaces have been prepared in a single step utilising three different maleic anhydride copolymers (so as to systematically investigate the role of polymer backbone structure), Scheme 1. These comprised poly(ethylene-*alt*-maleic anhydride) alternating copolymer as a reference standard (based on previously reported polyelectrolyte–fluorosurfactant switching studies[32]), poly(styrene-*alt*-maleic anhydride) where the aforementioned alternating copolymer ethylene segments are replaced with styrene segments, and finally poly(styrene-*co*-maleic anhydride) which is a copolymer consisting of single maleic anhydride units alternating with styrene block segments (because maleic anhydride does not homopolymerise[43]).

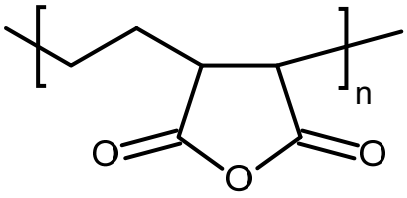

Poly(ethylene-*alt*-maleic anhydride)

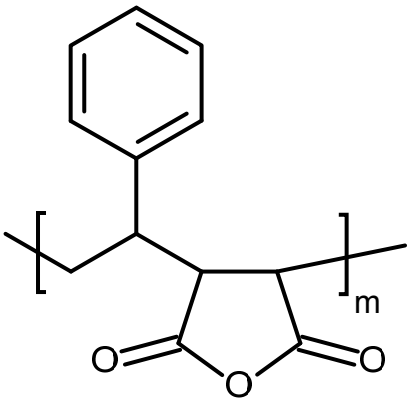

Poly(styrene-*alt*-maleic anhydride)

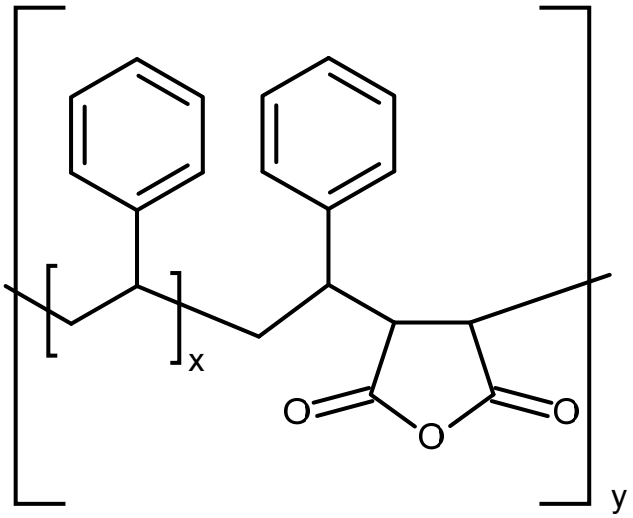

Poly(styrene-*co*-maleic anhydride)
(where x=0 for alternating copolymer)

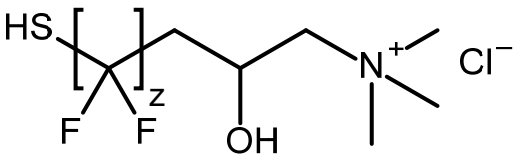

Zonyl® FSD cationic fluorosurfactant
(where z = 6–20)

Scheme 1: Maleic anhydride copolymers and cationic fluorosurfactant used to prepare copolymer–fluorosurfactant complexes.

2. EXPERIMENTAL

Polished silicon (100) wafers (Silicon Valley Microelectronics, Inc.) and glass slides (Academy Science Ltd.) were used as flat substrates. Poly(ethylene-*alt*-maleic anhydride) (poly(Et-*alt*-MA), Vertellus Specialties Inc.), poly(styrene-*alt*-maleic anhydride) (poly(St-*alt*-MA), Apollo Scientific Ltd.), or poly(styrene-*co*-maleic anhydride) (poly(St-*co*-MA), Polyscope Polymers BV) were dissolved in acetone (+99.8%, Sigma Aldrich Ltd.) at a concentration of 2% (w/v). The aqueous cationic fluorosurfactant (Zonyl® FSD, DuPont Ltd.) employed for complexation was further diluted in high purity water at a concentration of 5% (v/v) and then added to the copolymer solution resulting in hydrolysis of the maleic anhydride ring contained in the polymer leading to the formation of a polyelectrolyte–surfactant complex. The precipitated solid was collected from the liquid phase and dissolved at a concentration of 2% (w/v) in dimethylformamide (99%, Fisher Scientific UK Ltd.) for preparation of smooth surfaces and, in the case of the poly(St-*co*-MA)–fluorosurfactant complex, varying composition dimethylformamide–methanol (99%, Sigma Aldrich Ltd.) solvent mixtures were utilised to produce rough surfaces. Spin coating was carried out using a photoresist spinner (Cammax Precima) operating at 2000 rpm. For the oil–water separation experiments, stainless steel mesh (0.16 mm wire diameter, 0.20 mm square holes, The Mesh Company Ltd.) was dip coated in the copolymer–fluorosurfactant complex solution and the solvent allowed to evaporate.

Glass transition temperatures of the copolymer and copolymer–fluorosurfactant complexes were measured by differential scanning calorimetry (DSC, Pyris 1, Perkin Elmer Inc.).

Microlitre sessile drop contact angle analysis was carried out with a video capture system (VCA2500XE, AST Products Inc.) using 1.0 μL dispensation of de-ionised water (BS 3978 grade 1), hexadecane (99%, Sigma Aldrich Ltd.), tetradecane (+99%, Sigma Aldrich Ltd.), dodecane (99%, Sigma Aldrich Ltd.), decane (+99%, Sigma Aldrich Ltd.), octane (+99%, Sigma Aldrich Ltd.), heptane (99%, Sigma Aldrich Ltd.), hexane (+99%, Sigma Aldrich Ltd.), and pentane (+99%, Sigma Aldrich Ltd.). Advancing and receding contact angles were measured by respectively increasing and decreasing the droplet size until the contact line was

observed to move.[44] Oil repellency was further tested using motor engine oil (GTX 15W-40, Castrol Ltd.) and olive cooking oil (Tesco PLC). Switching parameters were determined by calculating the difference between equilibrium hexadecane and water contact angles.

Atomic force microscopy (AFM) images were collected in tapping mode at 20 °C in ambient air (Nanoscope III, Digital Instruments, Santa Barbara, CA) using a tapping mode tip with a spring constant of 42–83 N m^{-1} (Nanoprobe). Root-mean-square (RMS) roughness values were calculated over 100 x 100 μm scan areas consisting of 256 x 256 lines.

Anti-fogging was tested by exposing the coated surfaces to a high purity water spray from a pressurised nozzle (RG-3L, Anest Iwata Inc.).[45] Self-cleaning was tested by dispensing oil droplets onto a surface followed by rinsing with high purity water. Oil–water separation efficiencies were measured by pouring a vigorously agitated mixture of oil and water over stainless steel mesh which has been dip coated with copolymer–fluorosurfactant complex. The steel mesh was inclined at a shallow angle to allow the oil to roll off the mesh surface whilst the water passed straight through and the collected amounts were measured. Oil Red O (≥75% dye content, Sigma Aldrich Ltd) and Procion® Blue MX-R (35% dye content, Sigma Aldrich Ltd.) were employed as oil and water dispersible dyes respectively in order to enhance visual contrast (similar results were obtained in absence of dye). Oil–water separation efficiency was calculated from the volumes of liquid collected using the inclined coated meshes.

3. RESULTS

3.1 Surface Switching

Differential scanning calorimetry (DSC) showed that the poly(Et-*alt*-MA) copolymer has a higher glass transition temperature compared to the poly(St-*alt*-MA), which can be attributed to the larger molecular weight of the former and less ordering due to the stiff and bulky styrene groups[46] for the latter, Table 1. In the case of the poly(St-*co*-MA) copolymer, the presence of a single glass transition temperature is consistent with block styrene segments alternating with single maleic anhydride units (since a

plausible alternative diblock copolymer structure should display two respective glass transition temperatures[47]), Scheme 1. Also, its higher glass transition temperature compared to the poly(St-*alt*-MA) alternating copolymer stems from a combination of higher molecular weight and favourable intermolecular interactions between adjacent styrene units contained within the block styrene segments.[48]

Table 1: Glass transition temperatures of copolymers and copolymer–fluorosurfactant complexes.

Copolymer	Maleic Anhydride Unit Content / %	Molecular Weight / g mol^{-1}	Glass Transition Temperature / °C	
			Copolymer	Copolymer–Fluorosurfactant Complex
Poly(Et-*alt*-MA)	50	60,000	155	157
Poly(St-*alt*-MA)	50	50,000	120	131
Poly(St-*co*-MA)	26	80,000	160	138

Following fluorosurfactant complexation, both the poly(Et-*alt*-MA) and poly(St-*alt*-MA) copolymer–fluorosurfactant complexes display raised glass transition temperatures, which suggests a greater degree of ordering upon surfactant complexation, and is consistent with previous studies relating to copolymer–surfactant complex systems, Table 1.[49,50] In contrast, the glass transition temperature is lower for the poly(St-*co*-MA)–fluorosurfactant complex compared to that of the parent copolymer (and now fairly close to that of the alternating copolymer–fluorosurfactant complex); this may be due to disruption of the favourable intermolecular interactions between adjacent styrene units contained within the block segments (something which is absent for the parent alternating copolymers).[48,51]

Spin coating of all three copolymer–fluorosurfactant complexes dissolved in dimethylformamide (DMF) onto silicon wafers and glass slides produced smooth films (AFM RMS roughness = 1–5 nm), Table 2. In all cases, a time period of 10 s was sufficient for the water contact angles to reach their final static values, whilst hexadecane droplets remained stationary, Figure 1 and Table 2. In fact, both styrene-containing copolymer–fluorosurfactant complex surfaces reach a final static water contact angle value much faster than their ethylene-containing copolymer counterpart, with the poly(St-*alt*-MA)–fluorosurfactant system undergoing instantaneous water wetting. Copolymer–fluorosurfactant complex surfaces prepared using an alternative quaternary ammonium cationic fluorosurfactant (S-

106A, Chemguard) displayed similar oleophobic–hydrophilic switching behaviour. This was also found to be the case for copolymer–fluorosurfactant complex surfaces created using a cationic copolymer (poly(styrene-*alt*-maleimide), SMA® 1000I, Cray Valley HSC) and an anionic fluorosurfactant (Capstone® FS-63, Dupont Ltd). Repeat rinsing of samples in deionised water retained the observed oleophobic–hydrophilic behaviour. Control experiments utilising any of the parent copolymers (in the absence of fluorosurfactant complexation) showed the converse wetting behaviour, with an absence of superhydrophilicity and instantaneous spreading of hexadecane droplets, Table 2.

Table 2: Microlitre water and hexadecane static contact angles for copolymer spin coated from acetone solvent; copolymer–fluorosurfactant complex surfaces (smooth) spin coated from dimethylformamide (DMF) solvent; and poly(St-*co*-MA)–fluorosurfactant complex surfaces (rough) spin coated from 33 vol % DMF–66 vol % methanol. Water droplets were allowed to relax for 10 s to reach equilibrium prior to final static contact angle measurement. No relaxation in contact angle was observed for hexadecane droplets. AFM surface roughness values are included for comparison.

	AFM RMS Roughness / nm	**Static Water Contact Angle / °**		**Hexadecane Contact Angle / °**			
		0 s	**10 s**	**Static**	**Advancing**	**Receding**	**Hysteresis**
Poly(Et-*alt*-MA)	4.4±1	38±2	22±2	Wets	–	–	–
Poly(Et-*alt*-MA)–fluorosurfactant	1.1±0.3	88±2	<10	74±1	76±2	72±2	4±2
Poly(St-*alt*-MA)	6.7±1	68±2	66±2	Wets	–	–	–
Poly(St-*alt*-MA)–fluorosurfactant	2.7±0.3	<10	<10	80±2	85±2	66±2	19±2
Poly(St-*co*-MA)	10.3±1	90±2	90±2	Wets	–	–	–
Poly(St-*co*-MA)–fluorosurfactant	5.3±1	36±2	23±2	80±2	88±2	66±2	22±2

Poly(St-*co*-MA)–fluorosurfactant 33 vol % DMF–66 vol % methanol	246±3	<10	<10	112±5	125±5	<10	>115

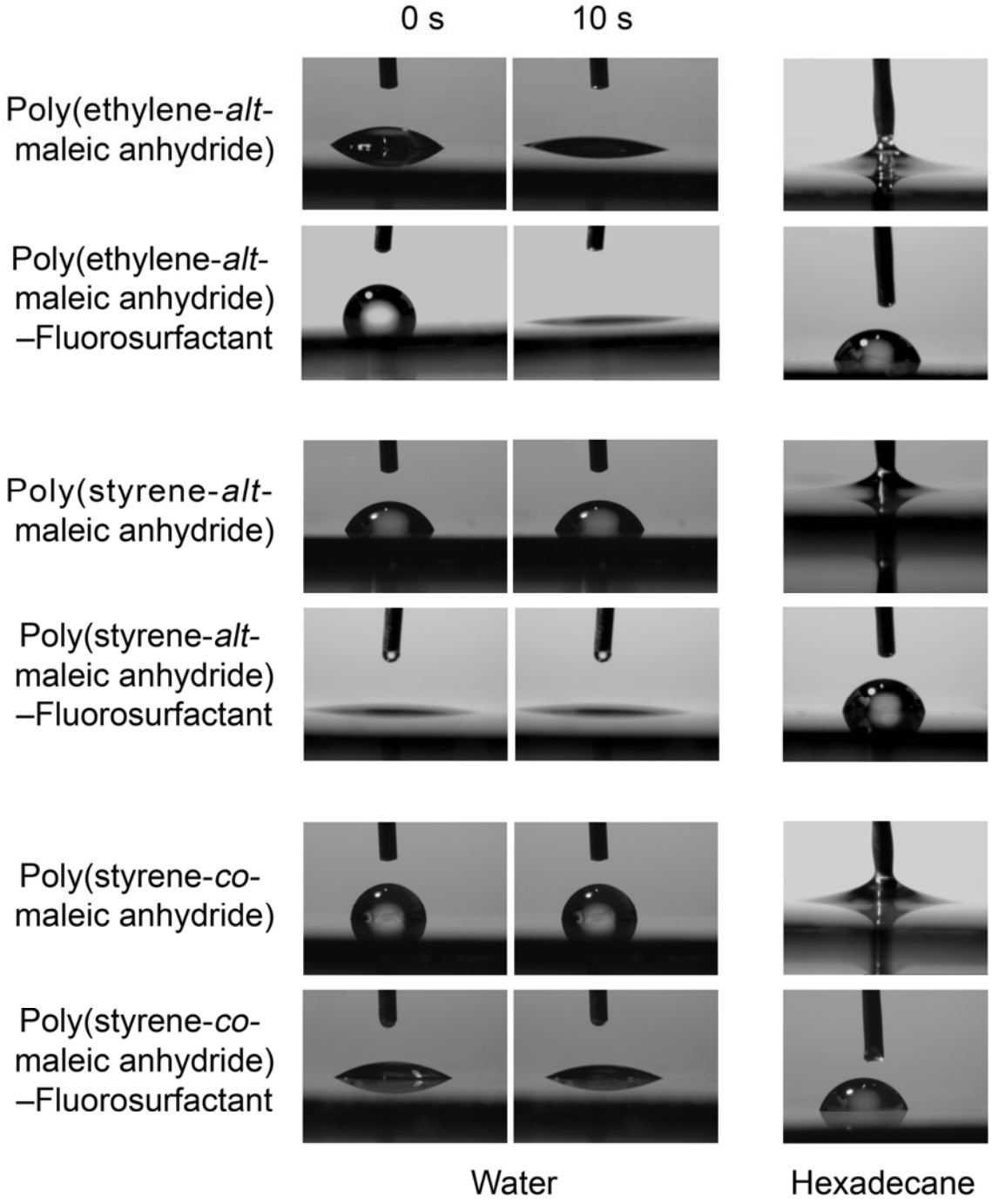

Figure 1: Microlitre water and hexadecane droplets dispensed onto copolymer spin coated from acetone solvent and copolymer–fluorosurfactant complex surfaces spin coated from dimethylformamide solvent. No relaxation in contact angle value was observed for hexadecane droplets.

Oil repellency of the poly(Et-*alt*-MA)–fluorosurfactant complex surfaces was found to improve (higher contact angle and lower hysteresis) with increasing

hydrocarbon length of straight chain alkane droplets, Figure 2. A similar trend was observed for both of the poly(styrene-maleic anhydride)–fluorosurfactant complex surfaces. Furthermore, olive oil and motor engine oil spreading were shown to be inhibited on all three types of copolymer–fluorosurfactant complex surfaces, Figure 3.

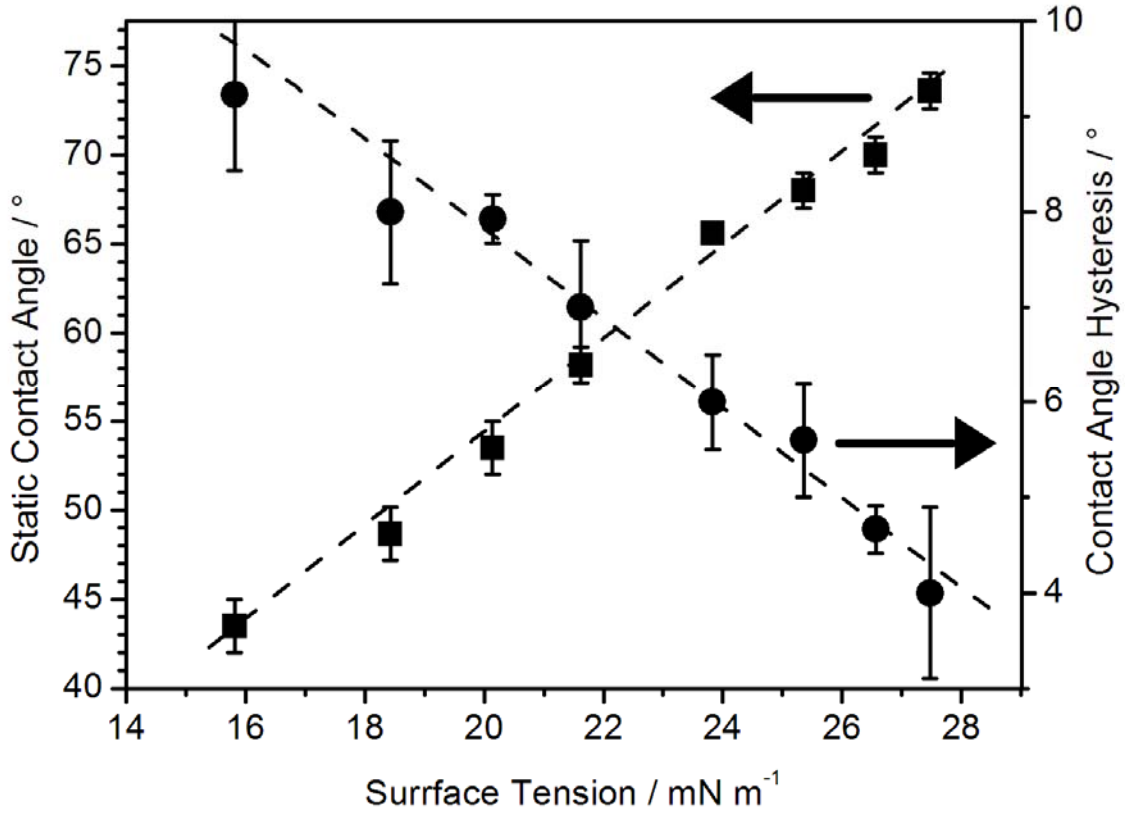

Figure 2: Microlitre droplet oil static contact angles and contact angle hysteresis on poly(Et-*alt*-MA)–fluorosurfactant complex surfaces spin coated from dimethylformamide solvent as a function of liquid straight chain alkane surface tension. A similar trend was noted for poly(St-*alt*-MA)–fluorosurfactant and poly(St-*co*-MA)–fluorosurfactant surfaces spin coated from dimethylformamide solvent.

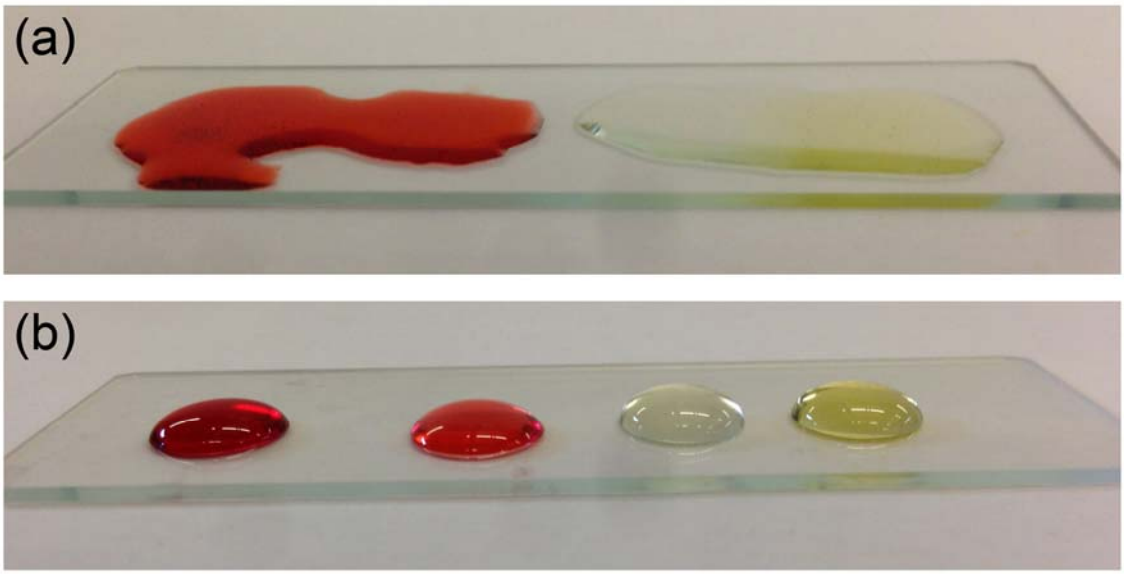

Figure 3: Hexadecane, octane, olive oil, and motor oil droplets (left to right) on: (a) uncoated glass slide; and (b) poly(Et-*alt*-MA)–fluorosurfactant complex surface solvent cast from dimethylformamide. A similar trend was noted for poly(St-*alt*-MA)–fluorosurfactant and poly(St-*co*-MA)–fluorosurfactant surfaces spin coated from dimethylformamide solvent. Hexadecane and octane droplets are dyed with Oil Red O (Sigma Aldrich Ltd.) to show contrast (similar results were obtained in the absence of dye).

3.2 Anti-Fogging and Self-Cleaning

Extremely low water contact angles are highly desirable for anti-fogging applications.[52] Copolymer–fluorosurfactant complex dip coated glass slides using dimethylformamide solvent were found to retain their transparency (anti-fogging) during liquid water spray exposure, Figure 4.

Figure 4: Demonstration of anti-fogging following exposure to water vapour (fogging): on uncoated glass slide and poly(Et-*alt*-MA)–fluorosurfactant complex solvent cast from dimethylformamide. Similar behaviour was observed for poly(St-*alt*-MA)–fluorosurfactant and poly(St-*co*-MA)–fluorosurfactant complex dip coated glass slides using dimethylformamide solvent.

Self-cleaning properties for the copolymer–fluorosurfactant dip coated glass slides were demonstrated by rinsing off fouling oils with just water, Figure 5. This is consistent with the high receding contact angle measured for hexadecane, Table 2.[53]

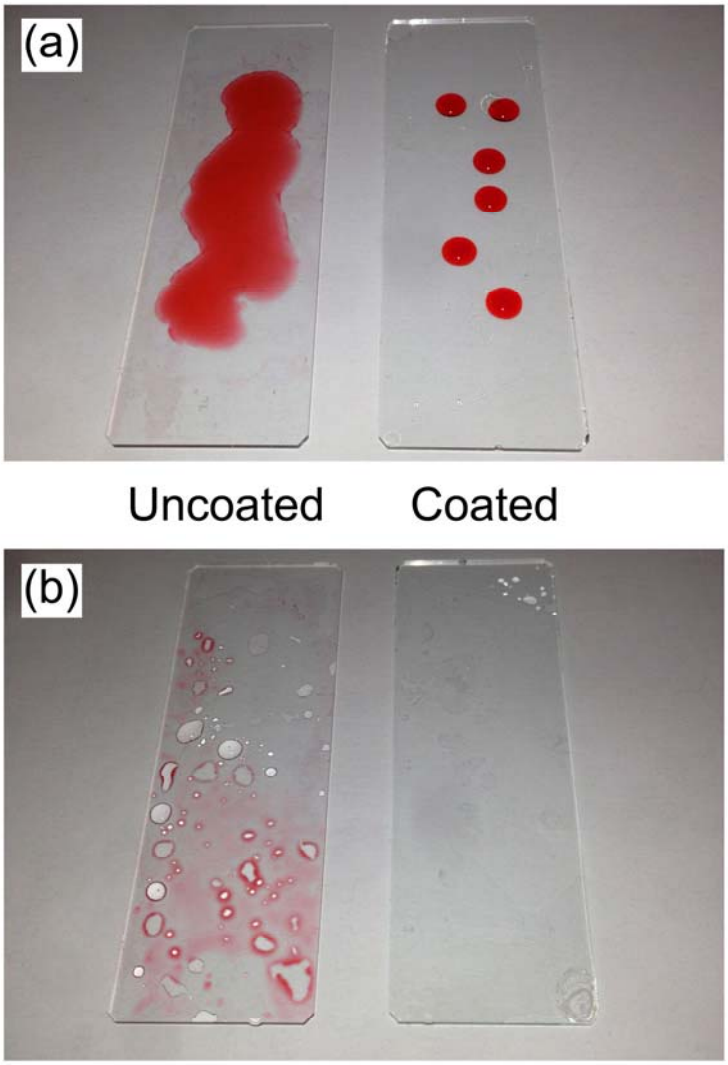

Figure 5: Demonstration of self-cleaning: (a) uncoated glass slide and poly(Et-*alt*-MA)–fluorosurfactant complex coating solvent cast from dimethylformamide fouled with hexadecane; and (b) after quick rinse with water. Similar behaviour was observed for poly(St-*alt*-MA)–fluorosurfactant and poly(St-*co*-MA)–fluorosurfactant complex surfaces solvent cast from dimethylformamide. Hexadecane droplets are dyed with Oil Red O (Sigma Aldrich Ltd.) to show contrast (similar results were obtained in the absence of dye).

3.3 Solvent-Induced Roughening to Enhance Switching Parameter

Further enhancement of the oleophobic–hydrophilic surface switching behaviour was investigated for the poly(St-*co*-MA)–fluorosurfactant system by varying the casting solvent mixture composition, Figure 6. Diluting dimethylformamide with methanol gives rise to an increase in surface roughness, which is attributable to the poor solubility of the styrene block segments in methanol.[54] This solvent-induced roughness lowers the static water contact angle (<10°) whilst concurrently raising the static hexadecane contact angle (>110°), to yield a hexadecane–water switching parameter exceeding 100°, Figures 6b and 6c. Control experiments showed a lack of surface roughness enhancement by varying the dimethylformamide–methanol solvent composition for poly(Et-*alt*-MA)–fluorosurfactant and the poly(St-*alt*-MA)–fluorosurfactant complex solutions, which is consistent with the absence of low methanol solubility styrene block segments being present in the alternating copolymer structures, Scheme 1.

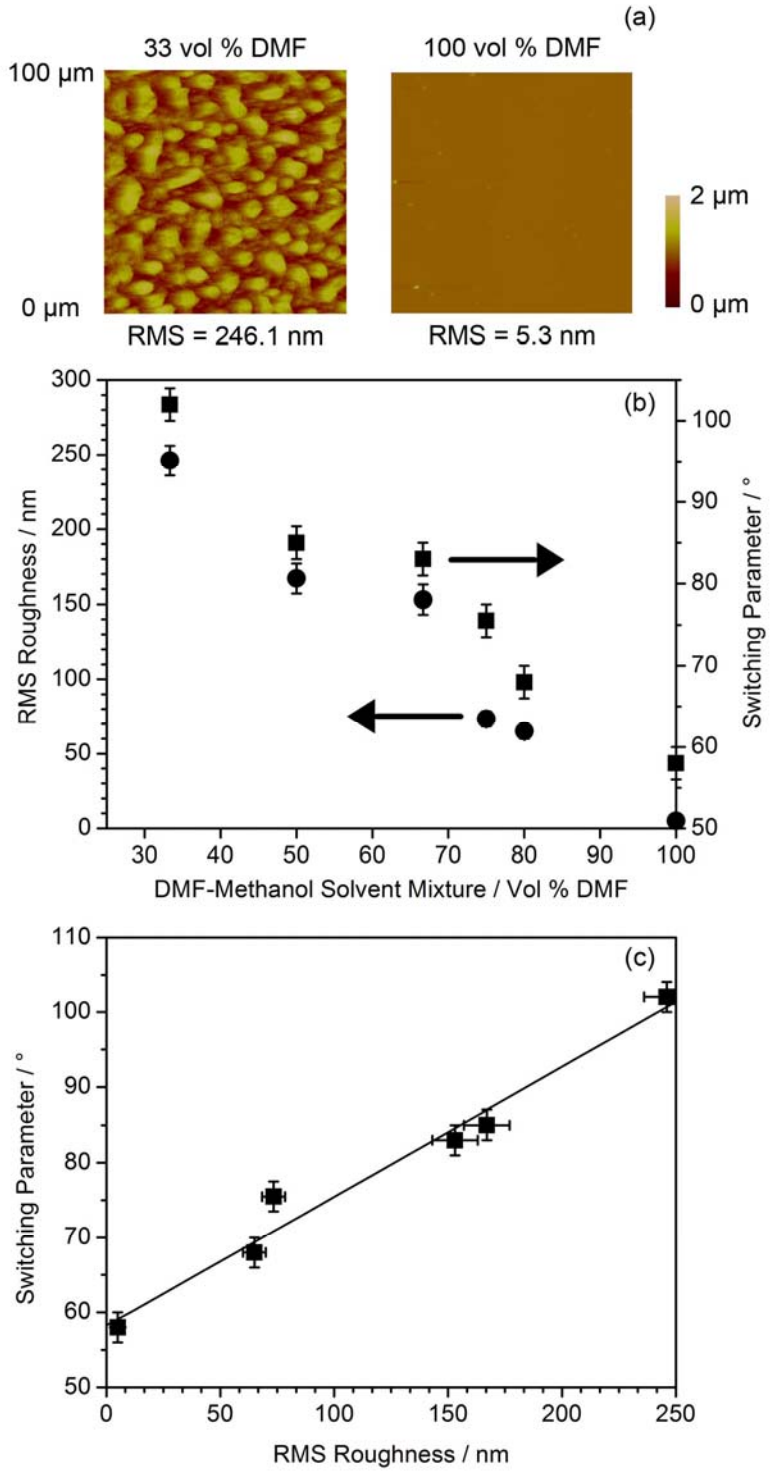

Figure 6: (a) AFM height images and RMS roughness values for poly(St-*co*-MA)–fluorosurfactant complex surfaces spin coated from different vol % dimethylformamide–methanol solutions; (b) AFM RMS roughness and hexadecane–water static contact angle switching parameter of poly(St-*co*-MA)–fluorosurfactant complex surfaces as a function of dimethylformamide–methanol solvent mixture composition; and (c) correlation between hexadecane–water static contact angle switching parameter of poly(St-*co*-MA)–fluorosurfactant complex surfaces and AFM RMS roughness.

3.4 Oil–Water Separation

Oil–water separation efficacy was tested using copolymer–fluorosurfactant complex coatings dip coated onto stainless steel mesh. These were then suspended over a sample vial followed by dispensing an agitated oil–water mixture. The water component was observed to pass through the mesh whilst the oil (hexadecane) remained suspended on the mesh surface, Figure 7. These meshes were then inclined at an angle, and pouring the agitated oil–water mixture over them yielded separation efficiencies as high as 98% in the case of the poly(St-*co*-MA)–fluorosurfactant complex surface (attributable to the dimethylformamide–methanol solvent mixture induced roughness enhancement of the oil–water switching parameter), Figure 7 and Table 3. Inclination of the meshes was required to allow the separated oil to flow downwards into an adjacent beaker. The absence of solvent induced roughness resulted in lower oil–water separation efficiencies for the two alternating copolymer–fluorosurfactant complex systems.

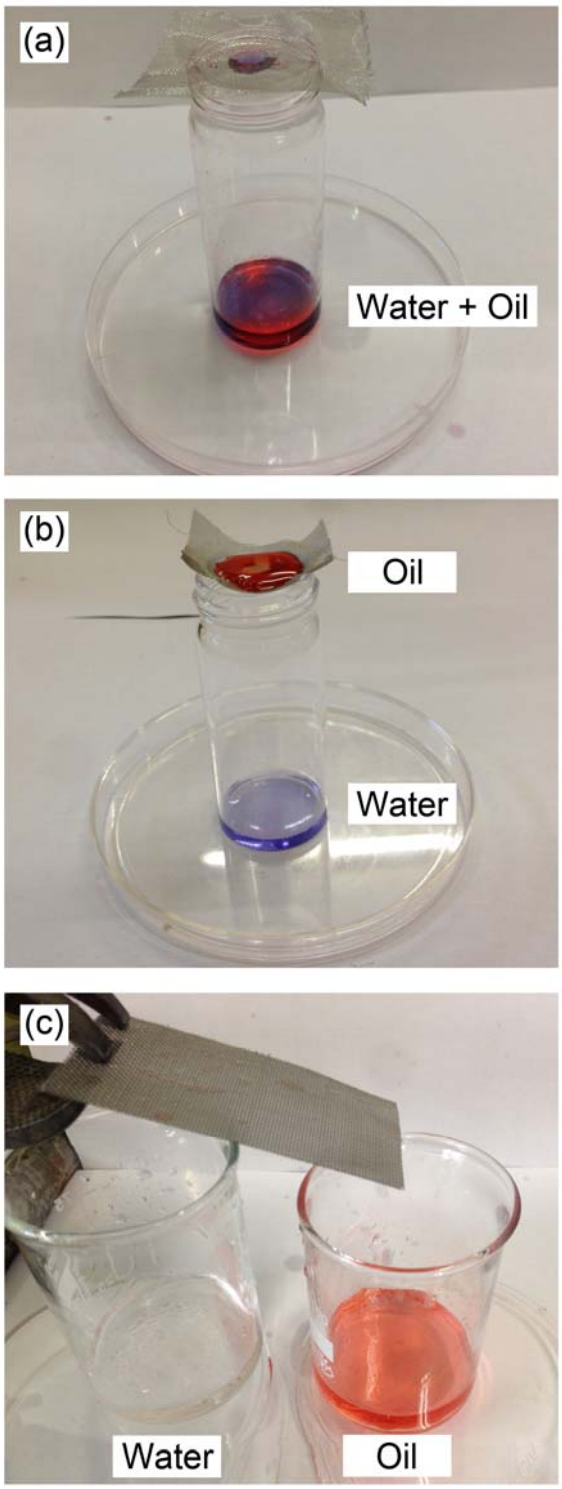

Figure 7: Demonstration of oil–water separation: agitated hexadecane–water mixture dispensed onto (a) uncoated stainless steel mesh; (b) stainless steel mesh dip coated with poly(St-*co*-MA)–fluorosurfactant complex in 33 vol % dimethylformamide–66 vol % methanol solvent mixture; and (c) inclined coated stainless steel mesh dip coated with poly(St-*co*-MA)–fluorosurfactant complex in 33 vol % dimethylformamide–66 vol % methanol solvent mixture acting as oil–water separator (oil and water are shown to be collected into separate beakers). Similar behaviour was observed for octane– and motor oil–water mixtures. Hexadecane is dyed with Oil Red O and water with Procion® Blue MX-R (in (a) and (b)) to show contrast (similar results were obtained in the absence of dye).

Table 3: Oil–water separation efficiencies using inclined meshes for copolymer–fluorosurfactant complex dip coated stainless steel mesh from 33 vol % dimethylformamide–66 vol % methanol solvent mixtures.

Switching Surface	AFM RMS Roughness / nm	Oil–Water Separation Efficiency[a] / %
Poly(Et-*alt*-MA) + fluorosurfactant	1.1±0.3	0
Poly(St-*alt*-MA) + fluorosurfactant	2.7±0.3	48±4
Poly(St-*co*-MA) + fluorosurfactant	246±3	98±2

[a]100% efficiency corresponds to complete separation of water from hexadecane.

4. DISCUSSION

Polymer–fluorosurfactant complex surfaces which display oleophobic–hydrophilic switching behaviour rely on the inherent hydrophilicity of the base polymer.[37] For instance, in the case of solvent cast ionic polymer–fluorosurfactant complex surfaces, the fluorinated surfactant tails segregate at the air–solid interface, thereby aligning the hydrolysed polymer counterionic groups and ionic surfactant heads towards the near-surface region as a consequence of their strong electrostatic attraction towards each other.[36,55,56] This interfacial interaction leads to an enhanced concentration of hydrophilic groups in the near-surface region. It has been proposed that such polymer–fluorosurfactant surfaces are able to exhibit oleophobic–hydrophilic switching behaviour due to the existence of defect sites or “holes” at the fluorinated surfactant tail air–solid interface through which water molecules can penetrate down towards the complexing counterion hydrophilic sub-surface.[37] This description helps to explain why all three copolymer–fluorosurfactant complex systems in the present study display lower final static water contact angles compared to their parent base copolymers, Figure 1 and Table 2.

The oleophobic–hydrophilic behaviour of such polymer–fluorosurfactant complex surfaces can be quantified in terms of a switching parameter (the difference in measured static contact angle between hexadecane and water droplets), Figure 8. Furthermore, it can be seen that the copolymer–fluorosurfactant complexes employed in the present study significantly outperform earlier reported switching surfaces in terms of this parameter. Most previous studies have tended to quote water contact angles only after allowing the droplet to stabilise over several minutes on the surface because of the slow rate at which water molecules penetrate through towards the hydrophilic sub-surface in order to manifest surface switching (although the surface initially is hydrophobic).[38,39,41] In the present investigation, the time taken to reach a final static water contact angle is much shorter (<10 s) for all copolymer–fluorosurfactant systems. Furthermore, both styrene-containing copolymer–fluorosurfactant complex surfaces reach a final static water contact angle value quicker than their ethylene-containing copolymer counterpart (and independently from surface roughness) due to the bulky styrene side group providing a lower packing efficiency for the former, and thereby facilitating a faster penetration of water into the hydrophilic sub-surface, Figure 1. This explanation is consistent with the styrene-based copolymer–fluorosurfactant complexes having lower glass transition temperatures, Table 1. In addition, for the case of the poly(St-*alt*-MA) copolymer, the more disordered nature of the alternating styrene side groups provides a greater level of polymer chain mobility,[57,58] which allows the fluorinated alkyl chains to reorient themselves more readily at the solid–air interface (culminating in instantaneous water wetting and high hexadecane contact angle values, Figure 1 and Table 2).

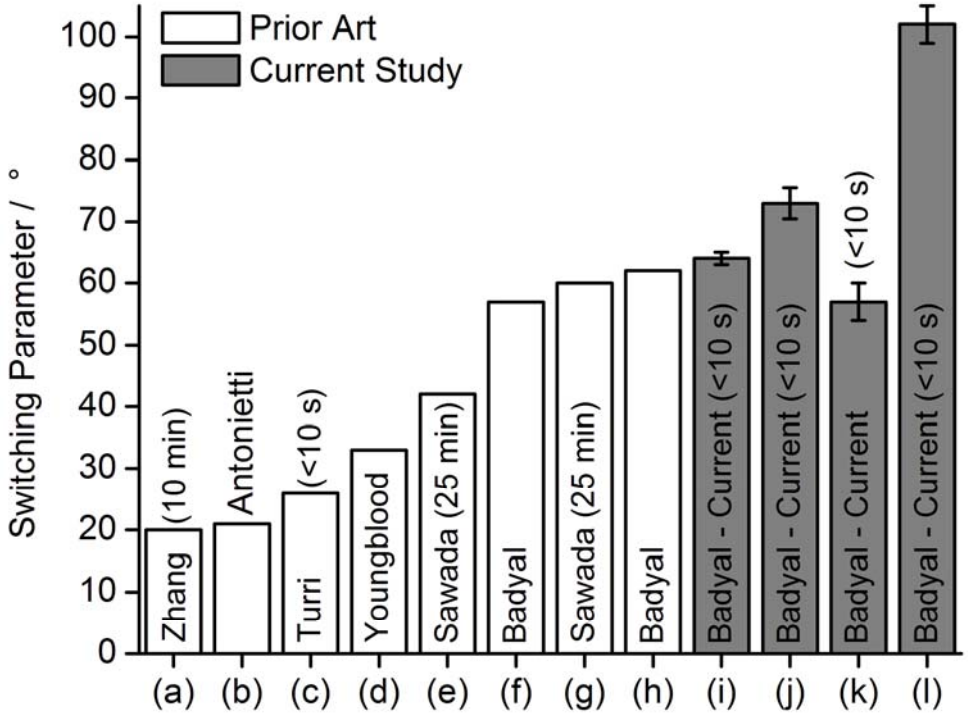

Figure 8: Oleophobic–hydrophilic switching parameters for nominally flat surfaces reported in the literature: (a) Zhang,[39] (b) Antonietti,[40] (c) Turri,[42] (d) Youngblood,[26] (e) Sawada,[38] (f) Badyal,[32] (g) Sawada,[41] (h) Badyal,[33] (i) poly(Et-*alt*-MA)–fluorosurfactant (RMS = 1.1±0.3 nm), (j) poly(St-*alt*-MA)–fluorosurfactant (RMS = 2.7±0.3 nm), (k) poly(St-*co*-MA)–fluorosurfactant (smooth RMS = 5.3±1 nm), and (l) poly(St-*co*-MA)–fluorosurfactant (rough RMS = 246±3 nm). Switching parameters are calculated from the difference between hexadecane and water static contact angles. Time taken for water to reach final static water contact angle value is given in brackets if reported.

The high receding hexadecane contact angle and low surface roughness of copolymer–fluorosurfactant complex surfaces spin coated from dimethylformamide solvent make them ideal for self-cleaning and anti-fog applications, Table 2 and Figures 3–5. Such surfaces are easily cleaned by rinsing in water (which replaces the oil–solid interaction with a much more favourable water–solid interaction, i.e. switching).

Dissolving the poly(St-*co*-MA)–fluorosurfactant complex in a dimethylformamide–methanol solvent mixture prior to film formation enhances surface roughness due to the poor solubility of the styrene block segments in methanol.[54] This surface roughness is capable of improving hydrophilicity due to increased surface area (Wenzel wetting[59]) and oleophobicity due to the ability to trap air (Cassie-Baxter wetting[60]), Table 2.[61,62,63] A key advantage of this approach is that it circumvents the need for introducing roughness as a separate step through the

incorporation of additional materials[39,61,64] or by mixing roughening particles into the copolymer–fluorosurfactant complex solution. It is envisaged that a range of different solvents or coating methods (e.g. spray coating[65]) may be used to introduce surface roughness for the enhancement of the switching parameter for related polymer–surfactant complex systems.

Coating of steel mesh with such roughened poly(St-*co*-MA)–fluorosurfactant complex surfaces (prepared from dimethylformamide–methanol solvent mixtures) provides hierarchical roughness (two length scales: steel mesh pores plus solvent-induced film roughness) both of which help to lower oil contact angle hysteresis (improve oil repellency).[66,67] When combined with the inherent high switching parameter, oil–water separation exceeding >98% efficiency is attained, Table 3. This performance matches existing oleophobic–hydrophilic systems for oil–water separation (which however tend to be far more complex in nature and fabrication methods).[3] Although there are more efficient separation processes (99.999% efficiency[68]) based on membrane filtration where small pores allow the passage of water whilst blocking oils,[69] such filters have low volume throughput and can be easily clogged with excess oil (thus requiring frequent cleaning or replacement). One embodiment of the current methodology would be to deploy it for pre-treatment filters installed upstream of conventional membrane filters, thereby ensuring removal of the majority of oil-based contaminants so as to minimise the amount of oil reaching the membrane filters (therefore avoid blockage as well as maximise efficiency). Such oil–water separators could potentially help to tackle the environmental impact of the gas, oil, metal, textile, and food processing industries.[70]

5. CONCLUSIONS

Solvent cast copolymer–fluorosurfactant complexes have been found to display large magnitude oleophobic–hydrophilic switching behaviour as well as rapid switching speeds. Further enhancement in switching performance is achieved by combining surface chemical functionality and roughness. These ultra-fast switching oleophobic–hydrophilic surfaces have been shown to display excellent anti-fog, self-cleaning, and oil–water separation properties.

6. ACKNOWLEDGEMENTS

We are grateful to Engineering and Physical Sciences Research Council (EPSRC – grant reference EP/J005401/1) and D Carswell for differential scanning calorimetry measurements.

7. REFERENCES

[1] Schaum, J.; Cohen, M.; Perry, S.; Artz, R.; Draxler, R.; Frithsen, J. B.; Heist, D.; Lorber, M.; Phillips, L. Screening Level Assessment of Risks Due to Dioxin Emissions from Burning Oil from the BP Deepwater Horizon Gulf of Mexico Spill. *Environ. Sci. Technol.* **2010**, *44*, 9383–9389.

[2] Cheng, Y.; Li, X.; Xu, Q.; Garcia-Pineda, O.; Andersen, O. B.; Pichel, W. G. SAR observation and model tracking of an oil spill event in coastal waters. *Mar. Pollut. Bull.* **2011**, *62*, 350–363.

[3] Kota, A. K.; Kwon, G.; Choi, W.; Mabry, J. M.; Tuteja, A. Hygro-responsive membranes for effective Oil–Water separation. *Nat. Commun.* **2012**, *3*, 1025.

[4] Kwon, G.; Kota, A. K.; Li, Y.; Sohani, A.; Mabry, J. M.; Tuteja, A. On-Demand Separation of Oil–Water Mixtures. *Adv. Mater.* **2012**, *24*, 3666–3671.

[5] Li, J.; Shi, L.; Chen, Y.; Zhang, Y.; Guo, Z.; Su, B.; Liu, W. Stable superhydrophobic coatings from thiol-ligand nanocrystals and their application in oil/water separation. *J. Mater. Chem.* **2012**, *22*, 9774–9781.

[6] Yang, H.; Lan, Y.; Zhu, W.; Li, W.; Xu, D.; Cui, J.; Shen, D.; Li, G. Polydopamine-coated nanofibrous mats as a versatile platform for producing porous functional membranes. *J. Mater. Chem.* **2012**, *22*, 16994–17001.

[7] Tian, D.; Zhang, X.; Tian, Y.; Wu, Y.; Wang, X.; Zhai, J.; Jiang, L. Photo-induced water–oil separation based on switchable superhydrophobicity–superhydrophilicity and underwater superoleophobicity of the aligned ZnO nanorod array-coated mesh films. *J. Mater. Chem.* **2012**, *22*, 19652–19657.

[8] Brown, V. J. Industry Issues: Putting the Heat on Gas. *Environ. Health Perspect.* **2007**, *115*, A76.

[9] Adebajo, M. O.; Frost, R. J.; Kloprogge, J. T.; Carmody, R.; Kokot, S. Porous Materials for Oil Spill Cleanup: A Review of Synthesis and Absorbing Properties. *J. Porous Mater.* **2003**, *10*, 159–170.

[10] Küntzel, J.; Ham, R.; Melin, Th. Regeneration of Hydrophobic Zeolites with Steam. *Chem. Eng. Technol.* **1999**, *22*, 991–994.

[11] Meininghuas, C. K. W.; Prins, R. Sorption of volatile organic compounds on hydrophobic zeolites. *Microporous Mesoporous Mater.* **2000**, *35–36*, 349.

[12] Alther, G. R. Organically modified clay removes oil from water. *Waste Manage.* **1995**, *15*, 623–628.

[13] Bayat, A.; Aghamiri, S. F.; Moheb, A.; Vakili-Nezhaad, G. R. Oil Spill Cleanup from Sea Water by Sorbent Materials. *Chem. Eng. Technol.* **2005**, *28*, 1525–1528.

[14] Teas, Ch.; Kalligeros, S.; Zanikos, F.; Stournas, S.; Lois, E.; Anastopoulos, G. Investigation of the effectiveness of absorbent materials in oil spills clean up. *Desalination* **2001**, *140*, 259–264.

[15] Annunciado, T. R.; Sydenstricker, T. H. D.; Amico, S. C. Experimental investigation of various vegetable fibers as sorbent materials for oil spills. *Mar. Pollut. Bull.* **2005**, *50*, 1340–1346.

[16] Sun, X.-F.; Sun, R.; Sun, J.-X. Acetylation of Rice Straw with or without Catalysts and Its Characterization as a Natural Sorbent in Oil Spill Cleanup. *J. Agric. Food Chem.* **2002**, *50*, 6428–6433.

[17] Radetić, M. M.; Jocić, D. M.; Jovančić, P. M.; Petrović, Z. L. J.; Thomas, H. F. Recycled Wool-Based Nonwoven Material as an Oil Sorbent. *Environ. Sci. Technol.* **2003**, *37*, 1008–1012.

[18] Zhu, Q.; Pan, Q.; Liu, F. Facile Removal and Collection of Oils from Water Surfaces through Superhydrophobic and Superoleophilic Sponges. *J. Phys. Chem. C* **2011**, *115*, 17464–17470.

[19] Feng, L.; Zhang, Z.; Mai, Z.; Ma, Y.; Liu, B.; Jiang, L.; Zhu, D. A Super-Hydrophobic and Super-Oleophilic Coating Mesh Film for the Separation of Oil and Water. *Angew. Chem. Int. Ed.* **2004**, *43*, 2012–2014.

[20] Wang, S.; Li, M.; Lu, Q. Filter Paper with Selective Absorption and Separation of Liquids that Differ in Surface Tension. *ACS Appl. Mater. Interfaces* **2010**, *2*, 677–683.

[21] Lee, C. H.; Johnson, N.; Drelich, J.; Yap, Y. K. The performance of superhydrophobic and superoleophilic carbon nanotube meshes in water–oil filtration. *Carbon* **2011**, *49*, 669–676.

[22] Jin, M.; Wang, J.; Yao, X.; Liao, M.; Zhao, Y.; Jiang, L. Underwater Oil Capture by a Three-Dimensional Network Architectured Organosilane Surface. *Adv. Mater.* **2011**, *23*, 2861–2864.

[23] Xue, Z.; Wang, S.; Lin, L.; Chen, L.; Liu, M.; Feng, L.; Jiang, L. A Novel Superhydrophilic and Underwater Superoleophobic Hydrogel-Coated Mesh for Oil/Water Separation. *Adv. Mater.* **2011**, *23*, 4270–4273.

[24] Howarter, J. A.; Youngblood, J. P. Amphiphile grafted membranes for the separation of oil-in-water dispersions. *J. Colloid Interface Sci.* **2009**, *329*, 127–132.

[25] Howarter, J. A.; Youngblood, J. P. Self-Cleaning and Anti-Fog Surfaces via Stimuli-Responsive Polymer Brushes. *Adv. Mater.* **2007**, *19*, 3838–3843.

[26] Howarter, J. A.; Genson, K. L.; Youngblood, J. P. Wetting Behavior of Oleophobic Polymer Coatings Synthesized from Fluorosurfactant-Macromers. *ACS Appl. Mater. Interfaces* **2011**, *3*, 2022–2030.

[27] Leng, B.; Shao, Z.; de With, G.; Ming, W. Superoleophobic Cotton Textiles. *Langmuir* **2009**, *25*, 2456–2460.

[28] Wang, Y.; Dong, Q.; Wang, Y.; Wang, H.; Li, G.; Bai, R. Investigation on RAFT Polymerization of a Y-Shaped Amphiphilic Fluorinated Monomer and Anti-Fog and Oil-Repellent Properties of the Polymers. *Macromol. Rapid Commun.* **2010**, *31*, 1816–1821.

[29] Briscoe, B. J.; Galvin, K. P. The effect of surface fog on the transmittance of light. *Sol. Energy* **1991**, *46*, 191–197.

[30] Xu, F. J.; Neoh, K. G.; Kang, E. T. Bioactive surfaces and biomaterials via atom transfer radical polymerization. *Prog. Polym. Sci.* **2009**, *34*, 719–761.

[31] Kobayashi, M.; Terayama, Y.; Yamaguchi, H.; Terada, M.; Murakami, D.; Ishihara, K.; Takahara, A. Wettability and Antifouling Behavior on the Surfaces of Superhydrophilic Polymer Brushes. *Langmuir* **2012**, *28*, 7212–7222.

[32] Lampitt, R. A.; Crowther, J. M.; Badyal, J. P. S. Switching Liquid Repellent Surfaces. *J. Phys. Chem. B* **2000**, *104*, 10329–10331.

[33] Hutton, S. J.; Crowther, J. M.; Badyal, J. P. S. Complexation of Fluorosurfactants to Functionalized Solid Surfaces: Smart Behavior. *Chem. Mater.* **2000**, *12*, 2282–2286.

[34] Goddard, E. D. Polymer–surfactant interaction part II. Polymer and surfactant of opposite charge. *Colloids Surf.* **1986**, *19*, 301–329.

[35] Thünemann, A. F.; Lochhaas, K. H. Surface and Solid-State Properties of a Fluorinated Polyelectrolyte–Surfactant Complex. *Langmuir* **1999**, *15*, 4867–4874.

[36] Vaidya, A.; Chaudhury, M. K. Synthesis and Surface Properties of Environmentally Responsive Segmented Polyurethanes. *J. Colloid Interface Sci.* **2002**, *249*, 235–245.

[37] Li, L.; Wang, Y.; Gallaschun, C.; Risch, T.; Sun, J. Why can a nanometer-thick polymer coated surface be more wettable to water than to oil? *J. Mater. Chem.* **2012**, *22*, 16719–16722.

[38] Sawada, H.; Yoshioka, H.; Kawase, T.; Takahashi, H.; Abe, A.; Ohashi, R. Synthesis and Applications of a Variety of Fluoroalkyl End-Capped Oligomers/Silica Gel Polymer Hybrids. *J. Appl. Polym. Sci.* **2005**, *98*, 169–177.

[39] Yang, J.; Zhang, Z.; Xu, X.; Zhu, X.; Men, X.; Zhou, X. Superhydrophilic-superoleophobic coatings. *J. Mater. Chem.* **2012**, *22*, 2834–2837.

[40] Antonietti, M.; Henke, S.; Thünemann, A. F. Highly ordered materials with ultra-low surface energies: Polyelectrolyte–surfactant, complexes with fluorinated surfactants. *Adv. Mater.* **1996**, *8*, 41–45.

[41] Sawada, H.; Ikematsu, Y.; Kawase, T.; Hayakawa, Y. Synthesis and Surface Properties of Novel Fluoroalkylated Flip-Flop-Type Silane Coupling Agents. *Langmuir* **1996**, *12*, 3529–3530.

[42] Turri, S.; Valsecchi, R.; Viganò, M.; Levi, M. Hydrophilic–oleophobic behaviour in thin films from fluoromodified nanoclays and polystyrene. *Polym. Bull.* **2009**, *63*, 235–243.

[43] Bartlett, P. D.; Nozaki, K. The Polymerization of Allyl Compounds. III. The Peroxide-induced Copolymerization of Allyl Acetate with Maleic Anhydride. *J. Am. Chem. Soc.* **1946**, *68*, 1495–1504.

[44] Johnson, R. E. Jr.; Dettre, R. H. In *Wettability*; Berg J. C., Ed.; Marcel Dekker, Inc.: New York, 1993; Chapter 1, pp 1–75.

[45] Mochizuki, C.; Hara, H.; Takano, I.; Hayakawa, T.; Sato, M. Application of carbonated apatite coating on a Ti substrate by aqueous spray method. *Mater. Sci. Eng., C* **2013**, *33*, 951–958.

[46] Kunal, K.; Robertson, C. G.; Pawlus, S.; Hahn, S. F.; Sokolov, A. P. Role of Chemical Structure in Fragility of Polymers: A Qualitative Picture. *Macromolecules* **2008**, *41*, 7232–7238.

[47] Kraus, G.; Childers, C. W.; Gruver, J. T. Properties of random and block copolymers of butadiene and styrene. I. Dynamic properties and glassy transition temperatures. *J. Appl. Polym. Sci.* **1967**, *11*, 1581–1591.

[48] López-Díaz, D.; Velázquez, M. M. Evidence of glass transition in thin films of maleic anhydride derivatives: Effect of the surfactant coadsorption. *Eur. Phys. J. E: Soft Matter Biol. Phys.* **2008**, *26*, 417–425.

[49] Kokufuta, E.; Zhang, Y.-Q.; Tanaka, T.; Mamada, A. Effects of Surfactants on the Phase Transition of Poly(N-isopropylacrylamide) Gel. *Macromolecules* **1993**, *26*, 1053–1059.

[50] Antonietti, M.; Conrad, J. Synthesis of Very Highly Ordered Liquid Crystalline Phases by Complex Formation of Polyacrylic Acid with Cationic Surfactants. *Angew. Chem. Int. Ed. Engl.* **1994**, *33*, 1869–1870.

[51] Ghebremeskel, A. N.; Vemavarapu, C.; Lodaya, M. Use of surfactants as plasticizers in preparing solid dispersions of poorly soluble API: Selection of polymer–surfactant combinations using solubility parameters and testing the processability. *Int. J. Pharm.* **2007**, *328*, 119–129.

[52] Grosu, G.; Andrzejewski, L.; Veilleux, G.; Ross, G. G. Relation between the size of fog droplets and their contact angles with CR39 surfaces. *J. Phys. D: Appl. Phys.* **2004**, *37*, 3350–3355.

[53] Howarter, J. A.; Youngblood, J. P. Self-Cleaning and Next Generation Anti-Fog Surfaces and Coatings. *Macromol. Rapid Commun.* **2008**, *29*, 455–466.

[54] Spatz, J. P.; Möller, M.; Noeske, M; Behm, R. J.; Pietralla, M. Nanomosaic Surfaces by Lateral Phase Separation of a Diblock Copolymer. *Macromolecules* **1997**, *30*, 3874–3880.

[55] Su, Z.; Wu, D.; Hsu, S. L.; McCarthy, T. J. Adsorption of End-Functionalized Poly(ethylene oxide)s to the Poly(ethylene oxide)–Air Interface. *Macromolecules* **1997**, *30*, 840–845.

[56] Walters, K. B.; Schwark, D. W.; Hirt, D. E. Surface Characterization of Linear Low-Density Polyethylene Films Modified with Fluorinated Additives. *Langmuir* **2003**, *19*, 5851–5860.

[57] Qiu, G.-M.; Zhu, L.-P.; Zhu, B.-K.; Xu, Y.-Y.; Qiu, G.-L. Grafting of styrene/maleic anhydride copolymer onto PVDF membrane by supercritical carbon dioxide: Preparation, characterization and biocompatibility. *J. Supercrit. Fluids* **2008**, *45*, 374–383.

[58] Reiter, G. Dewetting as a Probe of Polymer Mobility in Thin Films. *Macromolecules* **1994**, *27*, 3046–3052.

[59] Wenzel, R. N. Resistance Of Solid Surfaces To Wetting By Water. *Ind. Eng. Chem.* **1936**, *28*, 988–994.

[60] Cassie, A. B. D.; Baxter, S. Wettability of porous surfaces. *Trans. Faraday Soc.* **1944**, *40*, 546–551.

[61] Tuteja, A.; Choi, W.; Ma, M.; Mabry, J. M.; Mazzella, S. A.; Rutledge, G. C.; McKinley, G. H.; Cohen, R. E. Designing Superoleophobic Surfaces. *Science* **2007**, *318*, 1618–1622.

[62] Steele, A.; Bayer, I.; Loth, E. Inherently Superoleophobic Nanocomposite Coatings by Spray Atomization. *Nano Lett.* **2009**, *9*, 501–505.

[63] Choi, W.; Tuteja, A.; Chhatre, S.; Mabry, J. M.; Cohen, R. E.; McKinley, G. H. Fabrics with Tunable Oleophobicity. *Adv. Mater.* **2009**, *21*, 2190–2195.

[64] Tuteja, A.; Kota, A. K.; Kwon, G.; Mabry, J. M. Superhydrophilic and oleophobic porous materials and methods for making and using the same. U.S. Patent 20120000853 A1, Jan. 5, 2012.

[65] Badyal, J. P. S.; Woodward, I. S. Method and apparatus for the formation of hydrophobic surfaces. World Patent 2003080258 A2, Oct. 2, 2003.

[66] Gao, L.; McCarthy, T. J. The “Lotus Effect” Explained: Two Reasons Why Two Length Scales of Topography Are Important. *Langmuir* **2006**, *22*, 2966–2967.

[67] Zhao, H.; Park, K.-C.; Law, K.-Y. Effect of Surface Texturing on Superoleophobicity, Contact Angle Hysteresis, and “Robustness”. *Langmuir* **2012**, *28*, 14925–14934.

[68] Compass Water Solutions. http://www.cworldwater.com (accessed July 1, 2013).

[69] Hydration Technology Innovations. http://www.htiwater.com (accessed July 1, 2013).

[70] Cheryan, M.; Rajagopalan, N. Membrane processing of oily streams. Wastewater treatment and waste reduction. *J. Membr. Sci.* **1998**, *151*, 13–28.

TABLE OF CONTENTS GRAPHIC